Mon. Not. R. Astron. Soc. **000**, 000–000 (0000) Printed 24 July 2009 (MN LATEX style file v2.2)

The 21cm Power Spectrum After Reionization

J. Stuart B. Wyithe[1] and Abraham Loeb[2]
[1] *School of Physics, University of Melbourne, Parkville, Victoria, Australia*
[2] *Harvard-Smithsonian Center for Astrophysics, 60 Garden St., Cambridge, MA 02138*
Email: swyithe@unimelb.edu.au, loeb@cfa.harvard.edu

24 July 2009

ABSTRACT

We discuss the 21cm power spectrum (PS) following the completion of reionization. In contrast to the reionization era, this PS is proportional to the PS of mass density fluctuations, with only a small modulation due to fluctuations in the ionization field on scales larger than the mean-free-path of ionizing photons. We derive the form of this modulation, and demonstrate that its effect on the 21cm PS will be smaller than 1% for physically plausible models of damped Lyα systems. In contrast to the 21cm PS observed prior to reionization, in which HII regions dominate the ionization structure, the simplicity of the 21cm PS after reionization will enhance its utility as a cosmological probe by removing the need to separate the PS into physical and astrophysical components. As a demonstration, we consider the Alcock-Paczynski test and show that the next generation of low-frequency arrays could measure the angular distortion of the PS at the percent level for $z \sim 3-5$.

Key words: cosmology: diffuse radiation, large scale structure, theory – galaxies: high redshift, intergalactic medium

1 INTRODUCTION

Recently, there has been much interest in the feasibility of mapping the three-dimensional distribution of cosmic hydrogen through its resonant spin-flip transition at a rest-frame wavelength of 21cm (Furlanetto, Oh & Briggs 2007; Barkana & Loeb 2007). Several experiments are currently being constructed (including MWA [1], LOFAR [2], PAPER [3], 21CMA [4], GMRT [5]) and more ambitious designs are being planned (SKA [6]).

One driver for mapping the 21cm emission is the possibility of measuring cosmological parameters from the shape of the underlying power spectrum (PS; see Loeb & Wyithe 2008). During the epoch of reionization, the PS of 21cm brightness fluctuations is shaped mainly by the topology of ionized regions, rather than by the PS of matter density fluctuations which is the quantity of cosmological interest (McQuinn et al. 2006; Santos et al. 2007; Iliev et al. 2007). As a result, the line-of-sight anisotropy of the 21cm PS due to peculiar velocities must be used to separate measurements of the density PS from the unknown details of the astrophysics (Barkana & Loeb 2005; McQuinn et al. 2006). The situation is expected to be simpler both prior to the formation of the first galaxies (at redshifts $z \gtrsim 20$, Loeb & Zaldarriaga 2004; Lewis & Challinor 2007; Pritchard & Loeb 2008), and following reionization of the intergalactic medium (IGM; $1 \lesssim z \lesssim 6$) – when only dense pockets of self-shielded hydrogen, such as damped Lyα absorbers (DLA) and Lyman-limit systems (LLS) survive (Wyithe & Loeb 2008; Chang et al. 2007; Pritchard & Loeb 2008).

In this paper we focus our discussion on the post-reionization epoch (Wyithe & Loeb 2007; Chang et al. 2007). The DLAs which contain most of the neutral hydrogen mass in the Universe at $z \lesssim 6$ are expected to be hosted by galactic mass dark matter halos (Wolfe, Gawiser & Prochaska 2005). A survey of 21cm intensity fluctuations after reionization would measure the modulation of the cumulative 21cm emission from a large number of galaxies (Wyithe & Loeb 2008; Wyithe, Loeb & Geil 2008; Chang et al. 2007). Regarding the measurement of the 21cm PS, this lack of identification of individual galaxies is an advantage, since by not imposing a minimum threshold for detection, such a survey collects all the available signal. This point is discussed in Pen et al. (2008), where the technique is also demonstrated via measurement of the cross-correlation of galaxies with unresolved 21cm emission in the local Universe.

[1] http://www.haystack.mit.edu/ast/arrays/mwa/
[2] http://www.lofar.org/
[3] http://astro.berkeley.edu/ dbacker/EoR/
[4] http://web.phys.cmu.edu/ past/
[5] Pen et al. (2008)
[6] http://www.skatelescope.org/

Studying the 21cm PS after (rather than during) reionization offers two advantages. First, it is less contaminated by the Galactic synchrotron foreground, whose brightness temperature scales with redshift as $(1+z)^{2.6}$ (Furlanetto, Oh & Briggs 2006). Second, because the UV radiation field is nearly uniform after reionization, it should not imprint any large-scale features on the 21cm PS that would mimic the cosmological signatures. In addition, on large spatial scales the 21cm sources are expected to have a linear bias analogous to that inferred from galaxy redshift surveys.

Most previous studies of post-reionization 21cm fluctuations have assumed that the 21cm emission traces perturbations in the matter density, and have considered peculiar motions only after a spherical average (Wyithe & Loeb 2008; Pritchard & Loeb 2008, Loeb & Wyithe 2008). The exception is a recent paper discussing measurements of the dark energy equation of state (Chang et al. 2007). Since the neutral gas resides within collapsed dark matter halos, galaxy bias plays an important role in setting the 21cm fluctuation amplitude. In this paper we derive the 21cm PS after reionization in the context of the formalism that has been developed to calculate it during reionization (Barkana & Loeb 2005; McQuinn et al. 2006; Mao et al. 2008). By framing the derivation this way, the relative merits of cosmological constraints from 21cm surveys at redshifts before and after reionization can be more easily understood. In addition, this formalism provides a framework to describe the possible effect of fluctuations in the ionizing background. We then compute the Alcock-Paczynski effect (Alcock & Paczynski 1979) as an example for the cosmological utility of the post-reionization 21cm PS. In our numerical examples, we adopt the standard set of cosmological parameters (Komatsu et al. 2008), with values of $\Omega_{\rm b}=0.24$, $\Omega_{\rm m}=0.04$ and $\Omega_Q=0.76$ for the matter, baryon, and dark energy fractional density respectively, and $h=0.73$, for the dimensionless Hubble constant.

2 21CM POWER SPECTRUM AFTER REIONIZATION

The 21cm PS after reionization is expected to be dominated by the neutral content of galaxies. In a scenario where fluctuations in the ionizing background can be ignored, the form of the PS could therefore be inferred directly from the galaxy PS (Loeb & Wyithe 2008). However, we also include here the possible influence of a fluctuating ionizing background on the 21cm PS. Throughout our discussion, we assume the baryonic overdensity δ to equal the overdensity in dark-matter on sufficiently large scales.

2.1 The 21cm brightness temperature

The 21cm brightness temperature fluctuation in a region of IGM is

$$\Delta T = 23.8\left(\frac{1+z}{10}\right)^{\frac{1}{2}}\left[1-\bar{x}_i(1+\delta_x)\right](1+\delta)(1-\delta_v)\ {\rm mK}, \quad (1)$$

where $\delta_v=\partial v_r/\partial r(Ha)^{-1}$ and $\partial v_r/\partial r$ is the gradient of the peculiar velocity along the line-of-sight. The quantities $\bar{x}_i$ and δ_x are the mean ionization fraction and the fluctuation in ionization fraction, respectively. We have assumed that the spin temperature of hydrogen is much higher than the CMB temperature [as expected for collisionally coupled gas in collapsed objects, and observed in some DLAs (Curran et al. 2007)]. Thus we may neglect fluctuations in the kinetic and spin temperatures of the neutral hydrogen gas throughout the post reionization epoch. To evaluate the brightness temperature fluctuation we need to compute δ_x. With this goal in mind, we first write the fluctuation in neutral hydrogen fraction as

$$\delta_{\rm HI}\equiv x_{\rm HI}/\bar{x}_{\rm HI}-1, \quad (2)$$

where $\bar{x}_{\rm HI}$ and $x_{\rm HI}$ are the cosmic mean and local values for the neutral fraction (mass averaged).

2.2 Effect of the ionizing background

Next we compute the effect of the ionizing background on the neutral fraction. Two regimes must be considered.

2.2.1 Systems which are optically-thin to ionizing radiation

Low density regions of the Universe contain optically thin, Lyα absorbers. The ionization fraction in this regime is controlled by the balance between the ionization rate owing to the UV background and the recombination rate at the local gas density. Given an ionization rate Γ, and a hydrogen density $n_{\rm H}$ with a neutral fraction $x_{\rm HI}$, the equilibrium in the optically thin regime is given by the condition

$$x_{\rm HI}\sim\frac{n_{\rm H}\alpha_\beta}{\Gamma}, \quad (3)$$

where $\alpha_{\rm B}$ is the case-B recombination coefficient (Osterbrock & Ferland 2006). Assuming that the low density regions of the hydrogen density field are unbiased with respect to the underlying dark matter density, we have

$$x_{\rm HI}\propto(1+\delta-\frac{\Delta\Gamma}{\Gamma}), \quad (4)$$

where $\Delta\Gamma$ is the perturbation in the intergalactic ionizing background. Note that the neutral fraction in optically thin regions is increased in overdense regions by recombinations, and decreased by the presence of an excess ionizing background.

2.2.2 Optically-thick absorbers

Since optically-thick systems are self-shielded, the effect of the UV background on their ionization state depends on the gas distribution within them. Below we discuss the effect of an ionizing background on the HI content of self-shielded systems. Since most of the hydrogen in such systems is known to be contained within DLAs, we focus our discussion on DLAs.

The nature of DLAs is not understood, although they are thought to be formed by dense, self-shielded gas in galaxies (Wolfe, Gawiser & Prochaska 2005). The detailed modeling of DLAs is very uncertain, requiring numerical simulations that go beyond the scope of this paper. However we can utilise results of simulations in the literature to estimate the range of possible strength for the influence of the

UV background. The column density distribution of DLAs has a power-law form with a feature at $\sim 10^{20}\mathrm{cm}^{-2}$ (e.g. Storrie-Lombardi & Wolfe 2000). This feature has been interpreted by a number of authors as being due to the effects of self shielding of DLAs in a meta-galactic ionizing background (e.g. Corbelli, Salpeter & Bandiera 2001; Zheng & Mirada-Escude 2002).

Zheng & Mirada-Escude (2002) considered the column density distribution of damped Lyα systems modeled as spherical isothermal spheres. They solved for the self shielded HI density profile numerically and found that the neutral fraction reaches $\sim 10^{-3}$ at the radius where the system becomes optically thick to meta-galactic ionizing radiation. Their results demonstrate that the transition from highly ionized to highly neutral gas occurs over a narrow region which is very small compared with the size of the absorbing system. Moreover, they find that the radius $r_{\rm ss}$ at which the gas becomes self-shielding is proportional to $\Gamma^{-1/3}$. For a spherical isothermal sphere, the hydrogen mass enclosed within radius r scales as

$$M_{\rm H}(<r) \propto r, \tag{5}$$

and so the HI mass scales as

$$M_{\rm HI} = M_{\rm H}(<r_{\rm ss}) \propto r_{\rm ss} \propto \Gamma^{-1/3}. \tag{6}$$

We therefore find that a given perturbation in the ionizing background produces a corresponding perturbation in the mass of neutral hydrogen within the self-shielded system of the form

$$\frac{\Delta M_{\rm HI}}{M_{\rm HI}} = -\frac{1}{3}\frac{\Delta\Gamma}{\Gamma}. \tag{7}$$

Alternatively, the distribution of gas in a DLA may be better represented by a self-gravitating disk. The effect of a meta-galactic background on the ionization structure and starformation has been investigated by a number of authors (Corbelli, Salpeter & Bandiera 2001; Schaye 2004; Susa 2008). The hydrogen column depth at which the gas becomes self-shielding was shown to be proportional to $\Gamma^{1/3}$ as in the spherical isothermal case (Susa 2008). However the exponential profile of the disk models implies that the ionized portion of the gas contains much less mass than in the case of a more extended power-law isothermal profile. Corbelli, Salpeter & Bandiera (2001) compute the column depth of HI as a fraction of the column depth of hydrogen, at different intensities of ionizing background. For a disk with a column density of $10^{21}\mathrm{cm}^{-2}$, the fluctuation in HI mass owing to a fluctuation in the ionizing background is approximately

$$\frac{\Delta M_{\rm HI}}{M_{\rm HI}} \sim -2\times10^{-3}\frac{\Delta\Gamma}{\Gamma}. \tag{8}$$

This effect is two orders of magnitude smaller than in the case of a spherical isothermal sphere.

To evaluate the fluctuation in neutral fraction associated with DLAs we assume that the neutral gas is hosted within halos of mass M with associated galaxy bias b. We have[7]

$$x_{\rm HI} \propto \frac{(1+b\delta)(1-C\Delta\Gamma/\Gamma)}{1+\delta} \tag{9}$$

$$\sim 1+b\delta-\delta-C\frac{\Delta\Gamma}{\Gamma}, \tag{10}$$

where the last equality has reduced the expression to lowest order in δ.

2.2.3 Combined neutral content of the IGM

The above estimates of mass fluctuation suggest that the neutral hydrogen content of the IGM is modified owing to fluctuations in the ionizing background ($\delta_J \equiv \Delta\Gamma/\Gamma$) by a factor of the form

$$s \approx (1-C\delta_J), \tag{11}$$

where C is a constant describing the magnitude of the effect. For optically thin regions $C=1$, while for optically thick absorbers C can take a range of values. In the case of an isothermal sphere, a fluctuation in the ionizing background leads to a fluctuation in the HI mass of a self shielded system that is of comparable magnitude, indicating that the value of C in equation (11) would be of order unity in this case. However, in halos with virial temperatures larger than $\sim 10^4$K, hydrogen with an isothermal profile would be collisionally ionized, and hence have cooled into a much more concentrated profile. Since the host masses of DLAs are known to be greater than $10^{10}\mathrm{M}_\odot$ from clustering studies (Cook et al. 2006), an isothermal profile does not provide a physically plausible model. On the other hand, modeling DLAs using an exponential disk, as is appropriate for gas rich galaxies implies a much smaller value value of $C\sim10^{-3}$–10^{-2}. Thus, the effect of fluctuations in the ionizing background on the mass averaged HI density is expected to be small ($\lesssim 1\%$).

We can now add the effects of fluctuations in ionizing background on the neutral content of optically thin and optically thick absorbers within a region of large scale overdensity δ. We have

$$\begin{aligned} x_{\rm HI} &= F_{\rm thin}\bar{x}_{\rm HI}(1+\delta-\delta_J) + F_{\rm thick}\bar{x}_{\rm HI}(1+b\delta-\delta-C\delta_J) \\ &= \bar{x}_{\rm HI}\left[1+(F_{\rm thin}+F_{\rm thick}(b-1))\delta-(F_{\rm thin}+CF_{\rm thick})\delta_J\right] \\ &\sim \bar{x}_{\rm HI}\left[1+(b-1)\delta-C\delta_J\right], \end{aligned} \tag{12}$$

where $F_{\rm thin}$ and $F_{\rm thick}$ are the fractions of HI in the optically thin and optically thick regimes respectively. In the last equality, we assume the case where the optically thin component contains a negligible amount of the cosmic HI. Note that we ignore the optically thin component of the hydrogen in the remainder of this paper. However we point out that the inclusion of this additional component changes only the values of the co-efficients of δ and δ_J in the above equations, but not the form of the expression.

[7] The factor of $(1+\delta)$ in the denominator is present because this is the fluctuation in neutral hydrogen fraction rather than in neutral hydrogen mass.

2.2.4 Scale dependence of fluctuations in the ionizing background

Before deriving the fluctuation in neutral fraction we next need to calculate the dependence of the parameter δ_J on scale. Ionizing radiation in the IGM has a finite mean-free-path which increases with time following the end of reionization. On scales larger than the mean-free-path ($\lambda_{\rm mfp}$), with associated wavenumber $k < k_{\rm mfp} = 2\pi/\lambda_{\rm mfp}$, all ionizing photons within a fluctuation were produced by galaxies that were also within that fluctuation. In this case fluctuations in the ionizing background simply trace fluctuations in the density of galaxies so that the value of $\delta_J \propto b\delta$ is independent of scale. However, on scales smaller than the mean-free-path, ionizing photons were not produced by galaxies local to the fluctuation. As a result δ_J/δ is scale dependent.

To derive this dependence we convolve the real space density field with a filter function to account for the effects of finite mean-free-path and the inverse square dependence of ionizing flux. The fluctuation in flux at a position $\vec{x}$ becomes

$$\delta_J(\vec{x}) \propto \int d\vec{x}' G(\vec{x},\vec{x}')\delta(\vec{x}'). \quad (13)$$

For simplicity we assume that all ionizing photons travel one mean-free-path, hence

$$G(\vec{x},\vec{x}') = \frac{\Theta(|x-x'|-\lambda_{\rm mfp})}{|\vec{x}-\vec{x}'|^2}, \quad (14)$$

where Θ is the Heaviside step function. This may be rewritten

$$\delta_J(\vec{k}) \propto g(\vec{k})\delta_k, \quad (15)$$

where $\delta_J(\vec{k})$ and g are the Fourier transforms of the ionizing flux field and filter function respectively. We have

$$g(\vec{k}) \propto \frac{{\rm Si}(k\lambda_{\rm mfp})}{k}, \quad (16)$$

where

$${\rm Si}(x) = \int_0^x du \frac{\sin(u)}{u} \quad (17)$$

and $k = |\vec{k}|$. For small scales $k\lambda_{\rm mfp} \gg 1$, we obtain $\delta_J(k) \propto \delta_k/k$. For large scales we find $\delta_J(k) \propto \delta_k$ as expected from the argument described above.

Thus, we get the following dependence for the function s, which can now be written in terms of δ,

$$s(\delta) = \left[1 - K(k)b\delta\right], \quad (18)$$

where we have explicitly written in the galaxy bias (noting that it is the galaxy density rather than the matter density which sources the ionization field), and defined the function

$$K(k) = K_o\left(1+\frac{k}{k_{\rm mfp}}\right)^{-1}, \quad (19)$$

where $K_o \propto C$ is a new constant, which from the discussion following equation (11) is expected to be smaller than ~ 0.01. This fitting function interpolates smoothly between the limiting behaviour on small and large scales. We emphasise that this formulation is only valid on scales for which fluctuations in the density field are in the linear regime.

We can now express the fluctuation in the neutral hydrogen content, noting that this depends both on the density of galaxies and on the fluctuations in the ionizing background.

$$\delta_{\rm HI} \approx \left[b\left(1-K(k)\right)-1\right]\delta,$$

Similarly, we write the fluctuation in ionized fraction in terms of the local ionized hydrogen fraction (x_i) as

$$\delta_x \equiv x_i/\bar{x}_i - 1. \quad (20)$$

Using the fact that $x_i + x_{\rm HI} = 1$, we then find the ionization fluctuation in terms of the galaxy bias

$$\delta_x \approx \left[\bar{x}_{\rm HI}/(\bar{x}_{\rm HI}-1)\right]\left[b(1-K(k))-1\right]\delta. \quad (21)$$

2.3 The 21cm PS

We can now turn to calculating the 21cm PS. To lowest order in Fourier space, the velocity fluctuation may be written as, $\delta_v(\vec{k}) = -f\mu^2\delta$ where μ is the cosine of the angle between the $\vec{k}$ and line-of-sight unit vectors (Kaiser 1987), and[8] $f = d\log\delta/d\log(1+z)$. To leading order in δ, it then follows from equation (1) that the PS of brightness temperature fluctuations is given by,

$$\begin{aligned} P_{\Delta T} &= \mathcal{T}_{\rm b}^2\left[\left(\bar{x}_{\rm HI}^2 P_{\delta\delta} - 2\bar{x}_{\rm HI}(1-\bar{x}_{\rm HI})P_{\delta x} + (1-\bar{x}_{\rm HI})^2 P_{xx}\right)\right. \\ &\left. +2f\mu^2\left(\bar{x}_{\rm HI}^2 P_{\delta\delta} - \bar{x}_{\rm HI}(1-\bar{x}_{\rm HI})P_{\delta x}\right) + f^2\mu^4\left(\bar{x}_{\rm HI}^2 P_{\delta\delta}\right)\right] \quad (22) \end{aligned}$$

where $\mathcal{T}_{\rm b} = 23.8\left[(1+z)/10\right]^{\frac{1}{2}}$ mK, and $P_{\delta\delta}$, $P_{\delta x}$ and P_{xx} are the PS of density fluctuations, the PS of ionization fluctuations, and the cross-PS of ionization and density fluctuations respectively. Our expression for δ_x allows the ionization PS and ionization-density cross-PS to be related to the density PS in a very simple way

$$\begin{aligned} P_{\delta x} &= -\frac{\bar{x}_{\rm HI}}{1-\bar{x}_{\rm HI}}\left[b(1-K(k))-1\right]P_{\delta\delta} \\ P_{xx} &= \frac{\bar{x}_{\rm HI}^2}{(1-\bar{x}_{\rm HI})^2}\left[b(1-K(k))-1\right]^2 P_{\delta\delta}. \quad (23) \end{aligned}$$

In addition, the ionization PS and ionization-density cross-PS are very simply related to each other

$$P_{xx} = -\frac{\bar{x}_{\rm HI}}{(1-\bar{x}_{\rm HI})}[b(1-K(k))-1]P_{\delta x}. \quad (24)$$

Upon substitution of equation (23) into equation (22) we obtain an expression for the angular dependence of the post-reionization 21cm PS

$$P_{\Delta T}(b) = \mathcal{T}_{\rm b}^2\bar{x}_{\rm HI}^2\left[b(1-K(k))+f\mu^2\right]^2 P_{\delta\delta}. \quad (25)$$

Thus, when combined equations (22) and (23) provide a simple relation between the density PS and the 21cm PS involving ionization terms, allowing the full 21cm PS to be utilized in deriving cosmological constraints. This compares favorably with the reionization epoch, during which either the μ^4 term alone can be utilized (Barkana & Loeb 2005), or a functional form for the ionization PS must be assumed (Mao et al. 2008; Rhook et al. 2008). On large scales fluctuations in the ionization field will be correlated with density fluctuations. Thus fluctuations in ionizing background would be degenerate with the galaxy bias b. However, on small scales there is scale dependence in the function K which breaks the

[8] The quantity f is close to unity at high redshifts, taking values of 0.974, 0.988 and 0.997 at $z = 2.5$, 3.5 and 5.5.

degeneracy between ionization and galaxy bias. In addition, the angular dependence of the PS, which is due to gravitational infall and hence is independent of galaxy bias or ionization, breaks the degeneracy between galaxy bias and neutral fraction.

Equation (25) is valid on scales for which fluctuations are in the linear regime, and we can assume that galaxy bias is not scale dependent. In the case where $b = f = 1$ and $K_o = 0$ (i.e. unbiased sources at high redshift, with no modulation by the ionizing background) our expression for the PS reduces to the form of a uniformly ionized IGM, $P_{\Delta T}(b) = \mathcal{T}_{\rm b}^2 \bar{x}_{\rm H}^2 \left[1+\mu^2\right]^2 P_{\delta\delta}$ (Barkana & Loeb 2005). We note that in the absence of a modulation of power due to the ionizing background, equation (25) could have been derived directly from considering the galaxy PS (once it is realized that effect of a line-of-sight velocity is the same for the optical depth in the 21cm line and the galaxy number density).

Equation (25) is valid for a single halo mass. However the DLAs reside within halos having a range of masses. To account for this we define an unknown HI mass weighted probability density function $p(b)db$ for the galaxy bias. By substituting δ_x into equation (1), and integrating over $p(b)$ it is easy to show that the PS for an arbitrary distribution of bias is

$$P_{\Delta T} = \mathcal{T}_{\rm b}^2 \bar{x}_{\rm HI}^2 P_{\delta\delta} \left[\langle b\rangle(1-K(k)) + f\mu^2\right]^2 , \qquad (26)$$

where $\langle b\rangle$ is the mean of the bias distribution $p(b)$. For completeness we also calculate the spherically averaged PS

$$P_{\Delta T}^{\rm sph} = \mathcal{T}_{\rm b}^2 \bar{x}_{\rm HI}^2 P_{\delta\delta} \times \left[\langle b\rangle^2(1-K(k))^2 + \frac{2}{3} f\langle b\rangle(1-K(k)) + \frac{1}{5}f^2\right], \quad (27)$$

which, in the case of $\langle b\rangle = 1$, $f = 1$ and $K_o = 0$ reduces to the form for a uniformly ionized high redshift IGM, $P_{\Delta T}^{\rm sph} = 1.87 \times \mathcal{T}_{\rm b}^2 \bar{x}_{\rm HI}^2 P_{\delta\delta}$ (Barkana & Loeb 2005). Note that although the relation between neutral hydrogen mass and host halo mass is unknown, the PS depends only on the mean of $p(b)$. For later use we define $M_{\langle b\rangle}$ to be the halo mass corresponding to $\langle b\rangle$.

In Figure 1 we show examples of the dimensionless 21cm PS after reionization [$\Delta = k^3 P_{\Delta T}/(2\pi^2)$]. We assume $M_{\langle b\rangle} = 10^{11} M_\odot$, use the Sheth-Tormen fitting function for the bias (Sheth, Mo & Tormen 2001), and consider three redshifts, $z = 2.5$, $z = 3.5$ and $z = 5.5$, at which the mean-free-path for ionizing photons is taken to be $\lambda_{\rm mfp} = 600$, 300 and 100 co-moving Mpc, respectively (Bolton & Haehnelt 2007; Faucher-Giguere et al. 2008). There is at least a factor of 2 uncertainty in the value of the mean-free-path. However our results are insensitive to the exact value because the mean-free-path is larger than the scales accessible to 21cm PS observations (owing to the requirements of foreground removal) at all redshifts except those closest to reionization.

Two models are shown to illustrate the effect of the ionizing background on 21cm fluctuations. In the first we assume a fiducial model for which the ionizing background has no effect on the fluctuations in neutral fraction ($K_o = 0$). This is shown by the dotted curves in Figure 1. We also show examples of a model in which $K_0 = 1$, a value which is unphysically large but is chosen so as to clearly illustrate the qualitative effect of fluctuations in the ionizing background on the shape of the 21cm PS. In this model, the fluctuations in neutral fraction due to the ionizing background are as strong as (and hence cancel) the effect of the galaxy bias on large scales. Figure 1 illustrates that the fractional modulation of the 21cm PS is of order K_0, while as discussed in § 2.2.3, physically plausible values of K_0 are of order 10^{-2}. Since the fractional modification of the PS is of order $2K_0$, and our results indicate a fractional change in amplitude which is smaller than a factor of 2 at $k \sim 0.1$ over the redshift range considered, we therefore find that fluctuations in the ionizing background should modify the 21cm PS after reionization by $\lesssim 1\%$ on the scales and redshifts of interest.

2.4 Discussion

The effect of the ionizing background on the 21cm PS can be understood qualitatively as follows. Firstly, we have argued that the ionizing background follows the galaxy density field on large scales. As a result, on large scales regions of overdensity (underdensity) will have a higher (lower) than average ionizing background. In our linear formulation, the effect of the ionizing background is degenerate with galaxy bias on large scales, because in the case of $K_0 > 0$, it lowers (raises) the contribution to the 21cm intensity from galaxies with a particular halo mass. This modification of the 21cm intensity of galaxies reduces the amplitude of the PS, at all scales $k \ll k_{\rm mfp}$. We emphasise that because the fluctuations in the ionizing background are strongly correlated with density on large scales, they suppress rather than add additional power to the 21cm PS. The suppression becomes greater for smaller values of $k/k_{\rm mfp}$. Thus at fixed scale the effect of a fluctuating background is larger at higher redshift where the mean-free-path is smaller.

On small scales $k \gg k_{\rm mfp}$, only some fraction of the ionizing BG is produced locally within the fluctuation. The remainder of the ionizing background is generated within a region which averages over many fluctuations, and so has a mean value that is near that of the background. As a result, the suppression of power described above, owing to a correlation between the ionizing background and overdensity, is not as strong on small scales. Our derivation yields the variation of the suppression with scale ($\propto k^{-1}$). It should be noted that our formulation ignores the possible Poisson contribution to fluctuations in the ionizing background due to quasars. Poisson fluctuations introduce additional power into the 21cm PS beyond the component associated with the underlying density field of galaxies. The effect of Poisson fluctuations could become important at low redshift ($z \lesssim 3$), where quasars contribute significantly to the ionizing background. We do not consider the possible Poisson contribution in the remainder of this paper which focuses on redshifts above the peak of quasar activity ($z \gtrsim 2.5$).

We emphasise that our derivation of the 21cm PS after reionization is only valid on scales where the density fluctuations are in the linear regime. It should therefore be noted that there are potential complications that arise due to non-linearities in the mass and velocity fields on small scales. Analysis of the galaxy PS derived from N-body simulations has shown (Seo & Eisenstein 2005) that the PS can be treated as linear on scales greater than 15 co-moving Mpc (i.e. $k_{\rm max} \lesssim 0.4{\rm Mpc}^{-1}$) at $z = 3.5$, increasing towards higher redshifts. However, weak oscillatory features in the PS, such as the baryonic acoustic oscillations, are suppressed on even larger scales because matter moves across distances

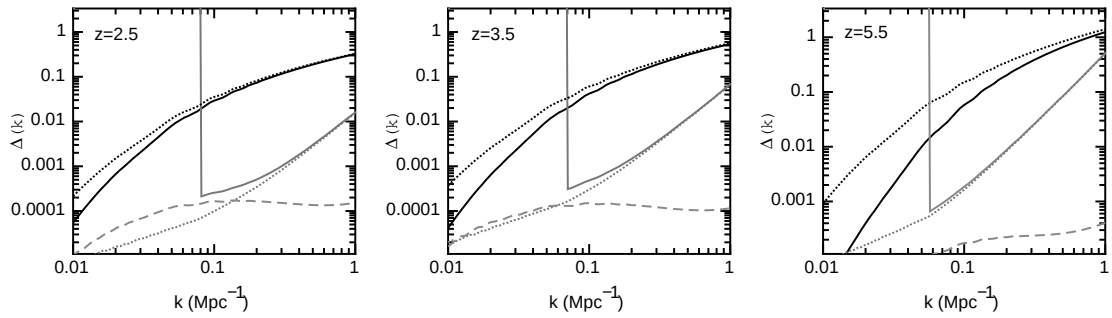

Figure 1. Examples of the post-reionization 21cm PS at three redshifts. Two cases are shown, assuming models with $K_o = 0$ (dotted curves) and $K_o = 1$ (solid curves). A DLA host mass of $M_{\langle b\rangle} = 10^{11} M_\odot$ was assumed at each redshift. The light solid curve shows the spherically averaged noise for the MWA5000, assuming 1000hr integration on each of three fields. The sharp upturn at low k is due to the assumption that foreground removal prevents measurement of the PS at scales corresponding to a bandpass larger than 8MHz. The thermal noise and cosmic variance (including the Poisson noise) components are plotted as the light dotted and light dashed curves respectively. The sensitivity curves are plotted within bins of width $\Delta k = k/10$.

on the order of $\sim$ 5–10Mpc over a Hubble time[9]. As groups of galaxies form, the linear-theory prediction for the location of each galaxy becomes uncertain, and as a result noise is added to the correlation among galaxies and hence to the measurement of the mass PS. The noise associated with the movement of galaxies smears out the acoustic peak in the correlation function of galaxies in real space (Eisenstein, Seo & White 2007; Seo, Siegel, Eisenstein & White 2008). The associated reduction of power in the baryonic acoustic oscillations is found to be in excess of 70% on scales smaller than $k_{\rm max} \sim 0.4{\rm Mpc}^{-1}$ at $z = 3.5$, corresponding to a length scale of $\sim \pi/(2k_{\rm max}) = 3.9$ comoving Mpc (Seo et al. 2008).

More importantly for experiments that aim to measure the PS shape is the non-linear correction to the PS due to virialised groups of DLAs (e.g., Tinker et al. 2006; Tinker 2007). The group velocity dispersion, $\sigma_{\rm vir}$, introduces the so-called "finger-of-god" in redshift space which is unrelated to the peculiar velocity according to linear theory. We can estimate the wavenumber at which this effect becomes important relative to the Hubble flow as, $k_{\rm vir} \sim \pi H(z)/(2\sigma_{\rm vir})$. At $z \sim 3.5$ we find $k_{\rm vir} \sim 10{\rm Mpc}^{-1}$. In the future, an improvement to our analysis could be made by including the analytic model for the redshift space galaxy two-point correlation function described by Tinker (2007). This model is constructed within the framework of the Halo Occupation Distribution, and quantifies galaxy bias on linear and non-linear scales. In addition, the model describes redshift-space distortions and clustering on both linear and non-linear scales. Finally, other non-linear effects may arise that are not present in galaxy redshift surveys, owing to internal rotation curve of the neutral hydrogen. However, the corresponding wave numbers are very large, $k \gg 10{\rm Mpc}^{-1}$.

[9] This characteristic scale of displacement follows from the fact that σ_8, the normalization of the power-spectrum on $8h^{-1}$Mpc, is of order unity at the present time.

2.5 sensitivity to the 21cm PS after reionization

Before proceeding to discuss the cosmological potential of the post-reionization 21cm PS, we compute the sensitivity with which it could be detected.

To compute the sensitivity $\Delta P_{\Delta T}(k,\mu)$ of a radio-interferometer to the 21cm PS, we follow the procedure outlined by McQuinn et al. (2006) and Bowman, Morales & Hewitt (2007) [see also Wyithe, Loeb & Geil (2008)]. The important issues are discussed below, but the reader is referred to these papers for further details. The uncertainty comprises of components due to the thermal noise, and due to sample variance within the finite volume of the observations. We also include a Poisson component due to the finite sampling of each mode (Wyithe 2008), since the post-reionization 21cm PS is generated by discrete clumps rather than a diffuse IGM. However we find that Poisson noise dominates only when $M_{\langle b\rangle} > 10^{11} M_\odot$ (see Wyithe 2008). We assume that foregrounds can be removed over 8MHz bins, within a bandpass of 32MHz (McQuinn et al. 2006) [foreground removal therefore imposes a minimum on the wave-number accessible of $k \sim 0.07[(1+z)/4.5]^{-1}{\rm Mpc}^{-1}$], and consider a hypothetical follow-up telescope to the MWA which would have 10 times the total MWA collecting area (we refer to this as the MWA5000). This telescope is assumed to have an antenna density distributed as $\rho(r) \propto r^{-2}$ within a diameter of 2km and a flat density core of radius 80m (see McQuinn et al. 2006). The antennae design is taken to be optimized at the redshift of observation (so that the physical collecting area of the array equals its effective collecting area), with each of 5000 phased arrays (tiles) consisting of 16 cross-dipoles. An important ingredient is the angular dependence of the number of modes accessible to the array (McQuinn et al. 2006). We assume 3 fields are observed for 1000 hr each. For the experiment described, the signal-to-noise of the PS will be largest over the decade of scales around $k \sim 0.1{\rm Mpc}^{-1}$ (McQuinn et al. 2006; Wyithe, Loeb & Geil 2008). The sensitivity curves (within bins of $\Delta k = k/10$) are plotted as the solid grey lines in Figure 1. We find that the both the 21cm PS, as well as the effect of a non-zero value of K_o would be easily measured using the MWA5000.

We note that the unprecedented power of cosmic-variance limited 21cm surveys for constraining cosmological parameters is made possible by the wide fields of view for the low-frequency telescopes under construction, combined with the very large volumes available at high redshift (Loeb & Wyithe 2008; Mao et al. 2008). For example, in units of the Sloan Digital Sky Survey volume ($\mathcal{V}_{\rm sloan} \sim 5.8 \times 10^8 {\rm Mpc}^3$) the telescope described would observe $\mathcal{V}/\mathcal{V}_{\rm sloan} \sim 4.8$, $\mathcal{V}/\mathcal{V}_{\rm sloan} \sim 7.6$ and $\mathcal{V}/\mathcal{V}_{\rm sloan} \sim 9.8$ per observing field, at $z = 2.5$, $z = 3.5$ and $z = 5.5$, respectively. These large volumes are obtained because of the very wide field of view available to an array with a design like the MWA. The array described would have a primary beam of $A_\theta \sim 2000$ square degrees.

3 APPLICATION OF THE ALCOCK-PACZYNSKI TEST

Like traditional galaxy redshift surveys, the observed 21cm PS is sensitive to only one underlying PS ($P_{\delta\delta}$), in addition to the 4 parameters, $\bar{x}_{\rm HI}$ and $\langle b \rangle$, $k_{\rm mfp}$ and K_o. These parameters are related to properties of DLAs and LLSs, and can be measured through independent means via quasar absorption line studies (particularly true for $\bar{x}_{\rm HI}$, $\langle b \rangle$ and $k_{\rm mfp}$). This situation should be contrasted with the reionization era where the observed 21cm PS is also sensitive to long range, non-gravitational fluctuations through $P_{\delta x}$ and P_{xx}. Provided that the non-linear evolution of the PS can be properly accounted for, this dominant dependence on the density PS provides a considerable advantage for the purposes of cosmological constraints.

To illustrate the potential for cosmological constraints from the anisotropy of the 21cm PS after reionization, we calculate the Alcock-Paczynski (AP) effect. Our approach is to specify the general result of Barkana (2006) for the distortion of the true PS [$P^{\rm t}_{\Delta T}(k,\mu)$] resulting from an incorrect choice of cosmology. This is parameterised in terms of the dilation parameters α and $\alpha_\perp$, which describe the distortions between the transverse and line-of-sight scales, and in the overall scale, respectively. These are defined such that $(1+\alpha)$ is the ratio between the assumed and true values of $(D_{\rm A}H)$, while $(1+\alpha_\perp)$ is the ratio between the assumed and true values of the angular diameter distance, $D_{\rm A}$. In the AP test, the correct cosmology is inferred by finding cosmological parameters for which $\alpha = \alpha_\perp = 0$.

To calculate the AP effect we apply equation (8) in Barkana (2006)

$$P_{\Delta T}(k,\mu) = (1+\alpha-3\alpha_\perp)P^{\rm t}_{\Delta T} + (\alpha\mu^2-\alpha_\perp)\frac{\partial P^{\rm t}_{\Delta T}}{\partial \ln k} + \alpha(1-\mu^2)\frac{\partial P^{\rm t}_{\Delta T}}{\partial \ln \mu} \quad (28)$$

to the PS in equation (26). Here the PS $P_{\Delta T}$ and $P^{\rm t}_{\Delta T}$ are evaluated at the observed $\vec{k}$. This procedure results in a modified PS that is related to the true density PS ($P^{\rm t}_{\delta\delta}$) via

$$\begin{aligned} P_{\Delta T}(k,\mu) &= \mathcal{T}_{\rm b}^2 \bar{x}_{\rm HI}^2 P^{\rm t}_{\delta\delta} \left(\langle b\rangle(1-K(k)) + f\mu^2\right)^2 \\ &\quad \times \left[(1+\alpha-3\alpha_\perp) + \frac{d\ln P^{\rm t}_{\delta\delta}}{d\ln k}(\alpha\mu^2-\alpha_\perp)\right] \\ &- \mathcal{T}_{\rm b}^2 \bar{x}_{\rm HI}^2 P^{\rm t}_{\delta\delta}(\langle b\rangle(1-K(k)) + f\mu^2) \\ &\quad \times \left[2\frac{k}{k_{\rm mfp}}\frac{-K(k)}{1+(k/k_{\rm mfp})}\langle b\rangle(\alpha\mu^2-\alpha_\perp) \right. \\ &\quad \left. - 4\alpha\left(1-\mu^2\right) f\mu^2\right]. \quad (29) \end{aligned}$$

Barkana (2006) expanded the general form of this equation to find the linear combinations of the true PS $P^{\rm t}_{\delta\delta}$, $P^{\rm t}_{\delta x}$ and $P^{\rm t}_{xx}$ which form the coefficients of terms containing μ^0, μ^2, μ^4 and μ^6. His result shows that in general, the parameter α (which corresponds to anisotropy) mixes $P^{\rm t}_{\delta\delta}$, $P^{\rm t}_{\delta x}$ and $P^{\rm t}_{xx}$. As a consequence, the μ^6 term, which arises through the AP effect, must be isolated in order to probe the anisotropy parameter α. On the other hand, equation (29) is sensitive only to $P^{\rm t}_{\delta\delta}$. As a result, the coefficients of all powers of μ in the post-reionization PS can be utilised in the AP effect to find the cosmological parameters that yield $\alpha = \alpha_\perp = 0$.

3.1 AP constraints on the PS

We next use equation (29) to calculate the permissible region of parameter space $\vec{p} = (\alpha, \alpha_\perp, \bar{x}_{\rm HI}, M_{\langle b\rangle}, K_o)$ around a true solution with PS $P^{\rm t}_{\delta\delta}$ and $\vec{p}_o = (0, 0, 0.02, 10^{11} M_\odot, 0)$. The fiducial value of $M_{\langle b\rangle}$ is chosen to lie in the middle of the mass range for DLAs measured from the cross-correlation analysis of Cook et al. (2006). We have assumed that the mean-free-path of ionizing photons is known a'priori, and do not fit it as a free parameter. As part of this procedure, we assume an estimate for the sensitivity of the future low-frequency interferometer described in § 2.5 to the 21cm PS [$\Delta P_{\Delta T}(k,\mu)$], and construct likelihoods

$$\ln \mathcal{L}(\vec{p}) = -\frac{1}{2}\sum_{k,\mu}\left(\frac{P_{\Delta T}(k,\mu,\vec{p}) - P^{\rm t}_{\Delta T}(k,\mu,\vec{p}_o)}{\Delta P_{\Delta T}(k,\mu)}\right)^2, \quad (30)$$

where the sum is over bins of k and μ. To estimate the constraints achievable via the AP effect, we modify the linear power spectrum to include the nonlinear erasure of the acoustic peaks based on the work of Eisenstein et al. (2006). Specifically, we use

$$P^{\rm t}_{\delta\delta}(k) = \left(P_{\delta\delta}(k) - P^{\rm smth}_{\delta\delta}(k)\right)\exp\left(-k^2\Sigma^2_{\rm nl}/2\right) + P^{\rm smth}_{\delta\delta}(k), \quad (31)$$

where $P^{\rm smth}_{\delta\delta}$ is the "no wiggle" form from Eisenstein & Hu (1999), and $\Sigma_{\rm nl} = 3.9[(1+z)/4.5]^{-1}$Mpc in the high redshift limit. In addition, to account for the possibility of non-linearity in the smooth PS at small scales we restrict our fitting to wave numbers $k_{\rm max} < 0.4{\rm Mpc}^{-1}$ (see § 2.4).

The results are shown in Figure 2 for three redshifts, $z = 2.5$, 3.5 and 5.5. Likelihood contours are shown at each redshift for the parameter sets $(\alpha, \alpha_\perp)$, $(\bar{x}_{\rm HI}, M_{\langle b\rangle})$ and $(K_o, M_{\langle b\rangle})$. For each set the likelihood is marginalised over the remaining 3 parameters assuming flat prior probabilities. The exception is $\bar{x}_{\rm HI} \approx 0.02 \pm 0.002$, which we have assumed to be known a'priori (with Gaussian errors) from future observations of quasar absorption spectra. The assumed uncertainty in $\bar{x}_{\rm HI}$ corresponds to a factor of ~ 2 improvement over existing measurements (Wolfe, Gawiser

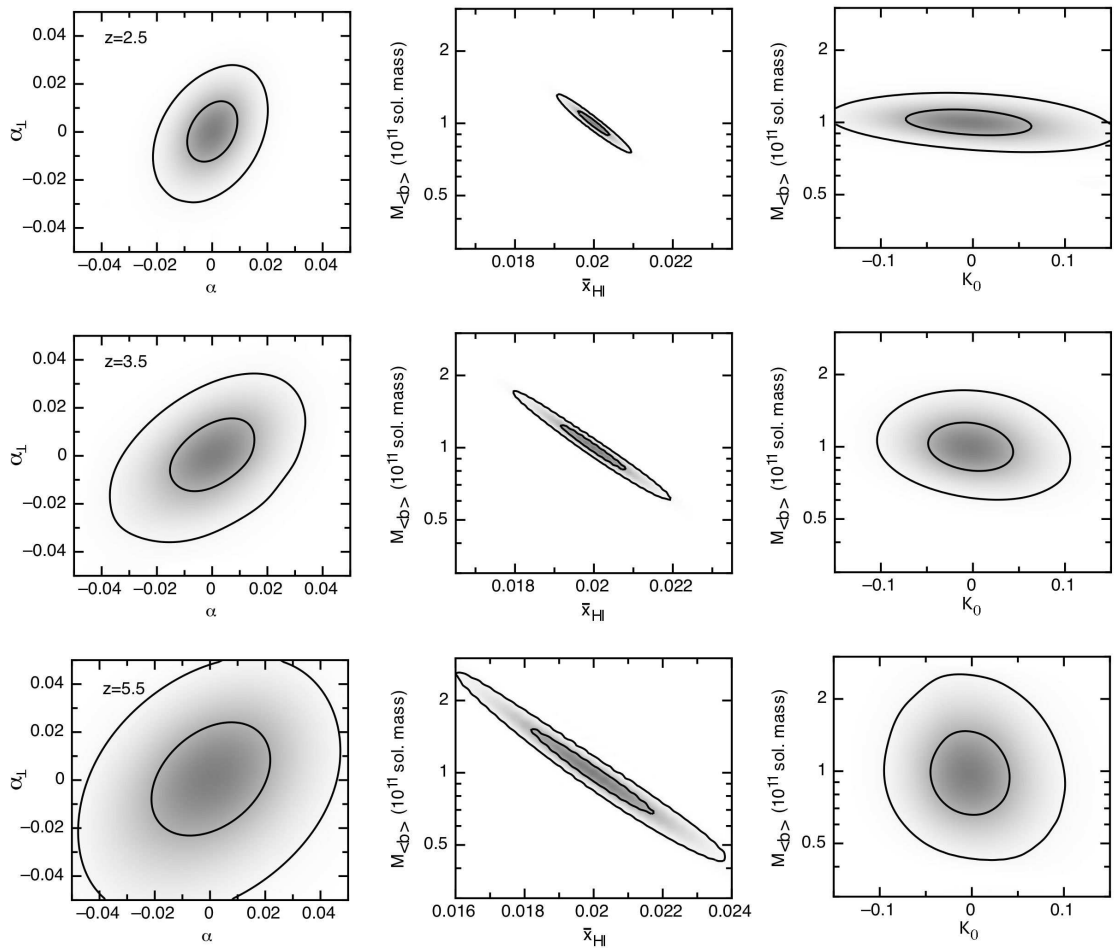

Figure 2. Constraints on the post-reionization PS distortions achievable via the AP test at 3 redshifts, assuming a fiducial model with $K_o = 0$. The three columns show parameter sets $(\alpha, \alpha_\perp)$, $(\bar{x}_{\rm HI}, M_{\langle b\rangle})$ and $(K_o, M_{\langle b\rangle})$. In each case likelihood contours are shown at 60% and 7% of the maximum likelihood. The projections of these contours onto individual parameter axes correspond to the 68.3% and 90% confidence ranges respectively.

& Prochaska 2005). Figure 2 shows that the angular dependence of the PS breaks degeneracy between the different parameters, allowing $\bar{x}_{\rm HI}$, $M_{\langle b\rangle}$, α, and $\alpha_\perp$ to each be measured from the fitting. In addition, the departure from the underlying shape of the PS allows the value of K_o to also be constrained.

We note that by including the uncertainties in the AP effect (through α and $\alpha_\perp$), our derived uncertainties for non-cosmological parameters ($M_{\langle b\rangle}$, $\bar{x}_{\rm HI}$ and K_o) include the uncertainty in the underlying matter power spectrum. An exception is that the uncertainty in the PS amplitude (which is proportional to the normalization of the primordial PS, σ_8) is degenerate with $\bar{x}_{\rm HI}$. However, since the error in $\bar{x}_{\rm HI}$ is comparable to or larger than the fractional error in σ_8, this does not add additional uncertainty relative to the constraints shown in Figure 2. An important additional uncertainty may also be introduced through the uncertainty in the primordial PS index or through a running spectral index, which we have not considered in this study.

At $z \lesssim 3.5$ the neutral fraction constraints are improved over the assumed prior information from the IGM. The mass of the DLA hosts is constrained to high precision (tens of percent, Wyithe 2008), with more accurate estimates at lower redshifts. In addition, the value of K_o is constrained to be smaller than a few hundredths (with minimal redshift dependence), although this in not at a level comparable to the physically expected value of $\sim 10^{-2}$. Thus, on scales larger than the mean-free-path, the perturbation due to the ionizing background ($\langle b\rangle K_o \delta$) is constrained at a level that is smaller than $\langle\delta^2\rangle^{1/2}$. On scales smaller than the mean free path, this perturbation is suppressed by $(k/k_{\rm mfp})^{-1}$. The cosmological constraints follow from the precision with which the distortion of the 21cm PS (as described by α and $\alpha_\perp$) can be measured. We find that distortions owing to the assumption of an incorrect cosmology could each be constrained at a percent level.

3.2 Comparison with high redshift constraints

Before concluding we show for comparison (Figure 3) the constraints on the parameter set $(\alpha, \alpha_\perp)$ for optimistic high redshift cases ($z = 12.5$ and 15), where we assume $\bar{x}_{\rm HI} = 1$ and fluctuations dominated by the density field ($P_{xx} = P_{\delta x} = 0$). These cases have fitted parameters

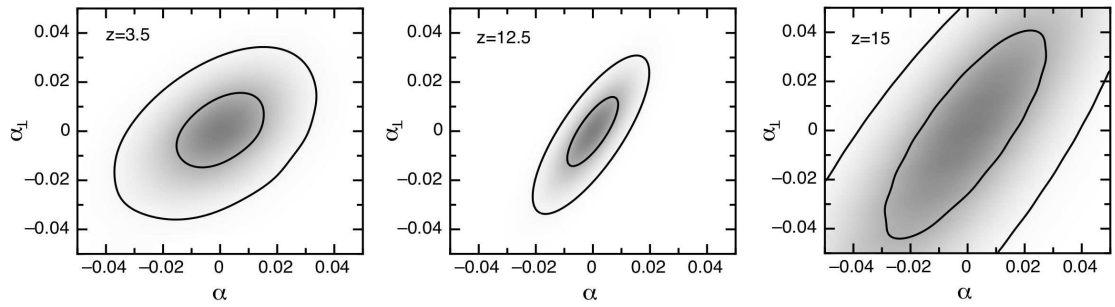

Figure 3. *Central and Right panels:* Constraints on the pre-reionization PS distortions achievable via the AP test at two redshifts. The results correspond to an optimistic high-redshift case, with $\bar{x}_{\rm HI} = 1$, and $P_{xx} = P_{\delta x} = 0$. The panels show the parameter set $(\alpha, \alpha_\perp)$. In each case, likelihood contours are shown at 60% and 7% of the maximum likelihood with each set marginalised over $\bar{x}_{\rm HI}$ (which we have assumed to be unconstrained a'priori). The projections of these contours onto individual parameter axes correspond to the 68.3% and 90% confidence ranges respectively. For comparison, (*left panel*) the $K_o = 0$ case at $z = 3.5$ is repeated from Figure 2.

$\vec{p} = (\alpha, \alpha_\perp, \bar{x}_{\rm HI})$, and correspond to the IGM prior to the formation of galaxies and ionized bubbles. The smaller $\bar{x}_{\rm HI}$ at $z < 6$ relative to the pre-reionization epoch is offset by the galaxy bias factor enhancement as well as the growth of structure, and by lower foreground contamination. With respect to constraining cosmological parameters, we find that the post-reionization 21cm PS would be competitive with the most optimistic expectations for the 21cm PS at high redshift.

4 CONCLUSIONS

In this paper we have derived the 21cm power spectrum (PS) following the completion of reionization. Our approach is to derive the PS within the formalism that has been developed to calculate the 21cm PS during reionization (Barkana & Loeb 2005; McQuinn et al. 2006; Mao et al. 2008). By framing the derivation this way we are able to directly compare the relative merits of cosmological constraints from 21cm surveys at redshifts prior to and post reionization. We have derived expressions for the components of the post-reionization 21cm PS that are due to the density field, the ionization field, and their cross-correlation. As is the case prior to reionization, we find that these components contribute to the observed PS in proportions that depend on the angle relative to the line-of-sight along which the power is measured. However, in difference from the situation prior to reionization, we have shown that all components of the 21cm PS are directly proportional to the PS of the underlying matter fluctuations, with a small but predictable modulation on scales below the mean-free-path of ionizing photons. We have derived the form of this modulation, and have shown that its effect on the observed PS will be at less than the 1% level for physically plausible astrophysical models of DLA systems. The simplicity of the 21cm PS after reionization stands in contrast to the astrophysical uncertainty during the reionization epoch, where HII regions dominate the 21cm signal. This simplicity will enhance the utility of the 21cm PS after reionization as a cosmological probe (Loeb & Wyithe 2008) by removing the need to separate the PS into physical and astrophysical components (Barkana & Loeb 2005).

To illustrate the utility of the 21cm PS after reionization as a cosmological probe, we have examined the Alcock-Paczynski (1979) test. Our calculations show that the next generation of low-frequency arrays could measure the angular distortion of the PS to around $\sim 1\%$ at $z \sim 3.5$. It has previously been shown that the scale of Baryonic Acoustic Oscillations, which constitutes a standard ruler (Blake & Glazebrook 2003; Seo & Eisenstein 2005; Eisenstein et al. 2005; Padmanabhan et al. 2007), can be also be used to independently probe H and $D_{\rm A}$ in 21cm PS, and hence to measure the equation of state of the dark energy (Wyithe, Loeb & Geil 2008; Chang et al. 2007). With the caveat that non-linear evolution of the 21cm PS must be quantitatively understood, our simple analysis indicates that the precision achievable via the Alcock-Paczynski (1979) test using the 21cm PS after reionization could be better than those available via a 21cm fluctuation measurement of the acoustic scale of baryonic oscillations for a given observing strategy (Shoji, Jeong & Komatsu 2009). More generally, our analysis shows that the 21cm PS after reionization shares the same favorable features as a galaxy redshift survey. The advantage of using 21cm fluctuations lies in the fact that individual sources need not be resolved. This would allow PS measurements using 21cm fluctuations to be extended to higher redshifts.

Acknowledgments. The research was supported by the Australian Research Council (JSBW), by NASA grants NNX08AL43G and LA, by FQXi, and by Harvard University funds (AL). We thank an anonymous referee for correcting an earlier error.

REFERENCES

Alcock C. & Paczynski, B., 1979, Nature, 281, 358
Barkana, R., 2006, Mon. Not. R. Astr. Soc., 372, 259
Barkana, R. & Loeb, A., 2007, Reports of Progress in Physics 70, 627.
Barkana, R. & Loeb, A., 2005, Astrophys. J. Lett. 624, L65
Blake C. & Glazebrook, K., 2003, Astrophys. J. 594, 665
Bolton, J. S., & Haehnelt, M. G. 2007, MNRAS, 382, 325
Bowman, J.D., Morales, M.F. & Hewitt, J.N., 2007, Astrophys. J., 661, 1

Chang, T.-C., Pen, U.-L., Peterson, J.B. & McDonald, P., 2007, ArXive-prints, 709, arXiv:0709.3672
Cooke, J., Wolfe, A. M., Gawiser, E., & Prochaska, J. X. 2006, ApJ, 652, 994
Corbelli, E., Salpeter, E. E., & Bandiera, R. 2001, ApJ, 550, 26
Curran, S.J., Tzanavaris, P., Pihlström, Y.M. & Webb, J.K., 2007, Mon. Not. R. Astron. Soc., 382, 1331
Eisenstein, D. J. et al., 2005, Astrophys. J. 633, 560
Eisenstein, D. J., & Hu, W. 1999, ApJ, 511, 5
Eisenstein, D. J., Seo, H.-J., & White, M. 2007, ApJ, 664, 660
Faucher-Giguere, C., Lidz, A., Hernquist, L., & Zaldarriaga, M. 2008, ArXiv e-prints, 807, arXiv:0807.4177
Furlanetto, S. R., Oh, S. P. & Briggs, F. H., 2006, Phys. Rep. 433, 181.
Iliev, I.T., Mellema, G., Pen, U.-L. & Shapiro, P.R., 2007, ArXiv e-prints, 712, arXiv:0712.1356
Kaiser, N., 1987, Mon. Not. R. Astron. Soc, 227, 1
Komatsu, E., et al. 2008, ArXiv e-prints, 803, arXiv:0803.0547
Lewis, A. & Challinor, A., 2007, Phys. Rev. D 76, 083005
Loeb, A. & Zaldarriaga, M., 2004, Phys. Rev. Lett. 92, 211301
Loeb, A. & Wyithe, J.S.B., 2008 Physical Review Letters, 100, 161301
Mao, Y., Tegmark, M., McQuinn, M., Zaldarriaga, M. & Zahn, O., 2008 ArXiv e-prints, 802, arXiv:0802.1710
McQuinn, M., Zahn, O., Zaldarriaga, M., Hernquist, L. & Furlanetto, S.R., 2006, Astrophys. J. 653, 815
Osterbrock, D. E., & Ferland, G. J. 2006, Astrophysics of gaseous nebulae and active galactic nuclei, 2nd. ed. by D.E. Osterbrock and G.J. Ferland. Sausalito, CA: University Science Books, 2006,
Padmanabhan, N. et al., 2007, Mon. Not. R. Astr. Soc., 378, 852
Pen, U.-L., Chang, T.-C., Peterson, J. B., Roy, J., Gupta, Y., & Bandura, K. 2008, The Evolution of Galaxies Through the Neutral Hydrogen Window, 1035, 75
Pen, U.-L., Staveley-Smith, L., Peterson, J. & Chang, T.-C., 2008, ArXiv e-prints, 802, arXiv:0802.3239
Pritchard, J.R. & Loeb, A., 2008, ArXiv e-prints, 802, arXiv:0802.2102
Rhook, K.J., Geil, P.M. & Wyithe, J.S.B., 2008, ArXiv e-prints, 803, arXiv:0803.2802
Santos, M.G., Amblard, A., Pritchard, J., Trac, H., Cen, R. & Cooray, A., 2007, ArXiv e-prints, 708, arXiv:0708.2424.
Schaye, J. 2004, ApJ, 609, 667
Shoji, M., Jeong, D., & Komatsu, E. 2009, ApJ, 693, 1404
Seo, H.-J. & Eisenstein, D.J., 2005, Astrophys. J. 633, 575
Seo, H.-J., Siegel, E. R., Eisenstein, D. J., & White, M. 2008, ArXiv e-prints, 805, arXiv:0805.0117
Shoji, M., Jeong, D., & Komatsu, E. 2008, ArXiv e-prints, 805, arXiv:0805.4238
Sheth, R.K., Mo, H.J. & Tormen, G., 2001, Mon. Not. R. Astron. Soc., 323, 1
Susa, H. 2008, ApJ, 684, 226
Tinker, J. L. 2007, MNRAS, 374, 477
Tinker, J. L., Weinberg, D. H., & Zheng, Z. 2006, MNRAS, 368, 85
Wolfe, A.M., Gawiser, E., & Prochaska, J.X., 2005, Ann. Rev. Astr. Astrophys. 43, 861
Wyithe, J.S.B. & Loeb, A., 2008 Mon. Not. R. Astr. Soc., 383, 606
Wyithe, J.S.B., Loeb, A. & Geil, P.M., 2008, Mon. Not. R. Astr. Soc., 383, 1195
Wyithe, S. 2008, ArXiv e-prints, 804, arXiv:0804.1624
Zheng, Z., & Miralda-Escudé, J. 2002, ApJL, 568, L71